Multilayered Balanced Wideband Bandpass Filter With High Filtering Selectivity

Li Yang
Dept. of Signal Theory and Communications
University of Alcalá
Alcalá de Henares, 28871 Madrid, Spain
li.yang@uah.es

Roberto Gómez-García
Dept. of Signal Theory and Communications
University of Alcalá
Alcalá de Henares, 28871 Madrid, Spain
roberto.gomezg@uah.es

***Abstract*—A type of multilayered balanced wideband bandpass filter (BPF) with high filtering selectivity is presented. It is composed of two back-to-back cascaded microstrip-to-microstrip vertical transitions using slotline stepped-impedance resonators (SIRs). Under differential-mode excitation, a sharp-rejection fifth-order wideband filtering transfer function with two paired close-to-passband transmission zeros can be attained in the proposed balanced BPF. Moreover, high common-mode suppression levels within the differential-mode passband range are achieved. For experimental-demonstration purposes, a microstrip prototype of the devised balanced wideband BPF architecture is developed and tested. It exhibits a measured differential-mode fifth-order high-selectivity wideband filtering response with center frequency of 4.015 GHz, 3-dB fractional bandwidth of 38.06%, and minimum in-band power-insertion-loss level of 0.947 dB. The common-mode suppression levels are above 20 dB from 2.075 to 5.588 GHz.**

Keywords—Balanced filter, bandpass filter (BPF), high selectivity, multilayered circuit, vertical transition, wideband filter.

I. Introduction

Owing to the intrinsic merit of immunity to common-mode noise, the development of balanced wideband bandpass filters (BPFs) and filtering circuits with high selectivity is always demanded by emerging RF wireless-communication systems with different functionalities [1]. Up to now, balanced wideband BPFs with remarkable common-mode suppression levels within their differential-mode passbands (e.g., [2] or [3]) and the whole frequency spectrum (e.g., [4]–[7]) have been conceived by using various design approaches and configurations. In [2], a balanced highly-selective wideband BPF was devised in a branch-line structure, whilst a wideband BPF with similar differential-mode response but poor common-mode suppression was realized with a balanced parallel-coupled-line topology in [3]. By exploiting double-sided parallel-strip lines and two 180° swap-structure-based phase shifters, a novel ultra-wideband differential BPF was presented in [4]. Next, differential wideband BPFs based on a T-shaped multi-mode microstrip resonator were studied in [5], but degraded common-mode responses were achieved within the in-band differential-mode frequency range. Furthermore, analytical discussions of a type of ultra-wideband differential BPFs shaped by wire-bonded multiconductor transmission lines were provided in [6]. In addition, by means of the multimode slotline resonator that features intrinsic common-mode-rejection behavior, wideband differential-mode BPFs were designed in [7]. However, the aforementioned balanced BPF devices suffer from one or two of the following performance drawbacks: (i) poor filtering selectivity and/or out-of-band power-attenuation levels under differential-mode excitation and (ii) degraded common-mode suppression within a limited frequency range.

In this paper, a two-layered balanced wideband BPF based on two back-to-back cascaded microstrip-to-microstrip vertical transitions is proposed. Unlike in the authors' previous study reported in [8], a fifth-order wideband high-selectivity filtering response under differential-mode excitation for the devised vertical transition using slotline stepped-impedance resonators (SIRs) is obtained. Meanwhile, a perceptible common-mode suppression action within the differential-mode passband range is attained, as studied with its equivalent circuit. For practical-validation purposes, a microstrip prototype of the engineered two-layered balanced wideband high-selectivity BPF centered at f_0 = 4 GHz is designed, fabricated, and characterized.

II. Design and Discussion

The equivalent transmission-line network of the proposed four-port balanced wideband BPF is depicted in Fig. 1(a). As shown, it is shaped by two microstrip-to-microstrip vertical transitions using slotline SIRs [8], which are back-to-back connected on the symmetry plane *A-A*'. Here, the back-to-back cascaded transmission-line sections and the additional shunt open-circuit-ended stubs attached at each port are designed with the same electrical length $\theta = 90°$ at $f_0/2$ (i.e., quarter-wavelength long at 2 GHz) but with different characteristic impedances Z_m and Z_{m1}. For the short-circuit-ended two-section transmission lines, their impedances are referred to as Z_{s1} and Z_{s2}, respectively, and the associated electrical lengths are set as $\theta_1 = \theta$ and $\theta_2 = \theta/2$. Moreover, Z_0 is the 50-Ω feeding-line impedance. In order to characterize the impedance variations of the coupled microstrip lines and the slotline in the practical electromagnetic (EM) simulation, two additional transformers with different turns ratios of N_m and N_s are employed [9].

Next, the differential- and common-mode properties of the suggested balanced wideband BPF are determined with $N_m = N_s = 1$. Its two-port equivalent circuit under differential-mode excitation is shown in Fig. 1(b), in which the back-to-back-connected transmission-line sections are virtually shorted at the symmetry plane. Note that, for the common-mode case, these two sections are open circuited due to the magnetic wall that results for that excitation. The relevant equivalent circuit is illustrated in Fig. 1(c). Based on the derived *ABCD* elements of the differential-mode circuit, a fifth-order wideband response centered at f_0 = 4 GHz is obtained, showing stopband-power-attenuation levels above 20 dB from 1.52 to 6.48 GHz (i.e., covering the passband range) as Fig. 2 depicts. Here, $Z_{s1} = Z_{s2}$ is selected. Meanwhile, in-band power-matching levels above 20 dB, as well as a sharp roll-off response that is attributed to the two paired close-to-passband transmission zeros, is attained. Here, compared to the conventional three-pole wideband vertical transition in [9], two additional transmission poles for the proposed differential-mode network are introduced by using two shunt open-circuit-ended stubs, which further enhance the sharpness

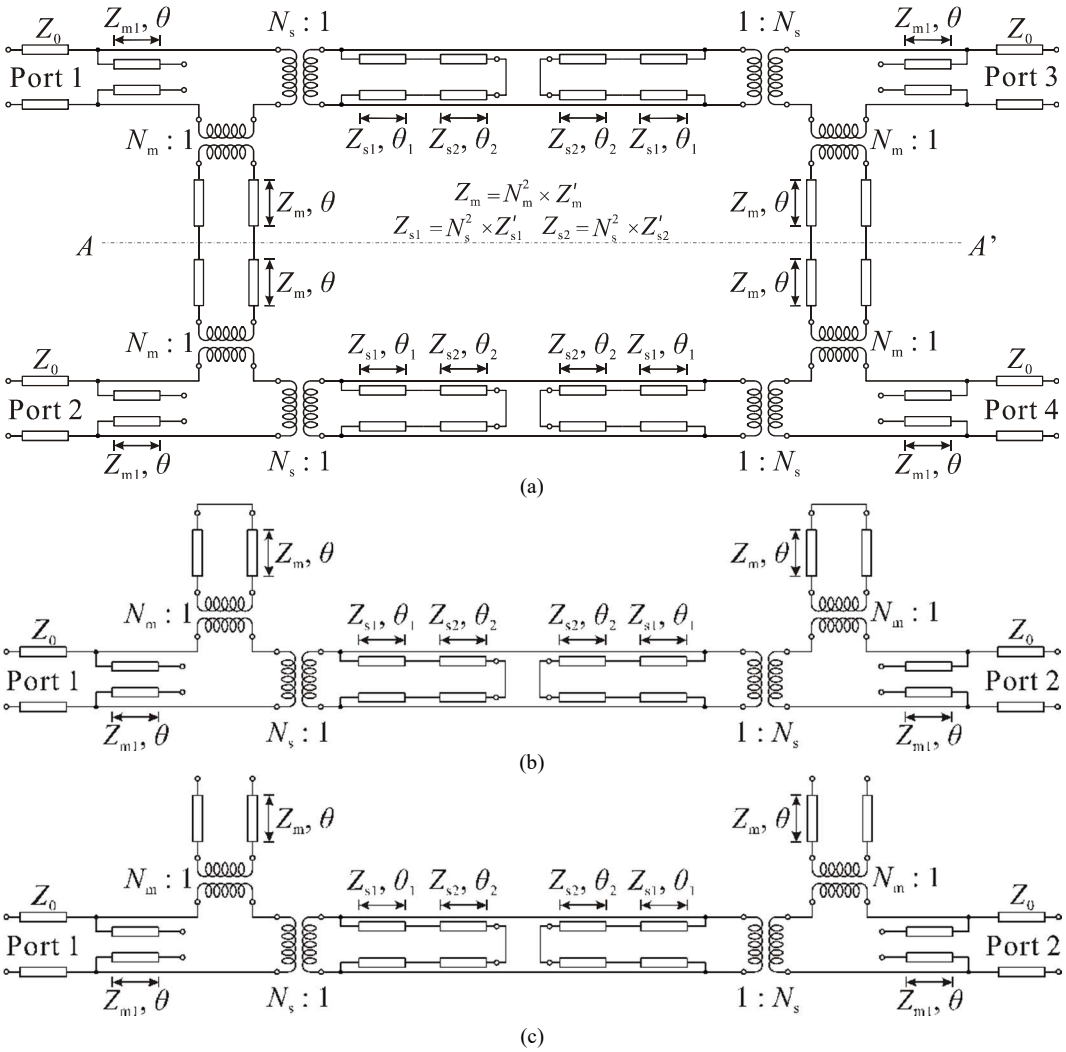

Fig. 1 Equivalent circuits of the proposed balanced wideband BPF based on two multilayered back-to-back-connected vertical transitions using slotline SIRs. (a) Equivalent circuit of the whole four-port balanced BPF network in which Port 1 and Port 2 and Port 3 and Port 4 are respectively paired as the input and output balanced ports. (b) Two-port differential-mode equivalent circuit. (c) Two-port common-mode equivalent circuit.

of the wideband BPF response. On the other hand, common-mode suppression levels higher than 30 dB from 2.39 to 5.61 GHz, which fully covers the frequency range of the differential-mode passband, can be achieved. It must be noticed that the common-mode suppression levels of this proposed balanced BPF are also increased by these two employed shunt open-circuit-ended stubs when compared to those without them.

III. Experimental Results

To experimentally verify the viability of the proposed balanced wideband BPF, a proof-of-concept prototype in a two-layered microstrip structure is developed, manufactured, and tested. A Roger's 4003C substrate with relative dielectric constant ε_r = 3.55, dielectric thickness h = 0.813 mm, and dielectric loss tangent of 0.0027 is employed. Fig. 3 depicts the layout of the conceived balanced wideband BPF, for which the back-to-back connected transmission-line sections, the shunt open-circuit-ended stubs, and the short-circuit-ended two-section transmission lines shown in Fig. 1 are respectively represented by the back-to-back cascaded microstrip-line sections, the shunt open-circuit-ended microstrip lines, and the slotline SIRs. The proposed wideband BPF was initially designed with Z_m = 116.2 Ω, Z_{m1} = 33.3 Ω, and Z_{s1} = Z_{s2} = 55.112 Ω, and it is simulated with Z'_m = 122.3 Ω, Z_{m1} =

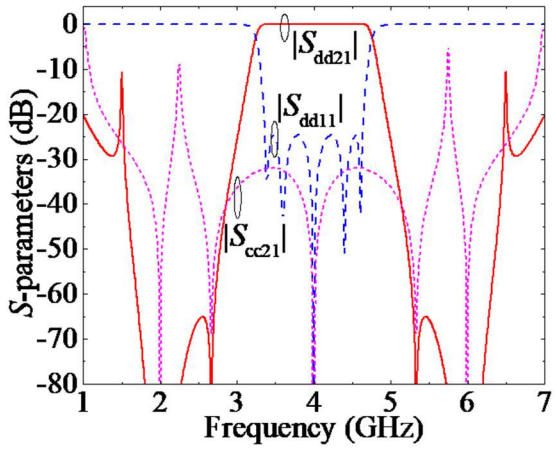

Fig. 2 Theoretical differential-mode power transmission ($|S_{dd21}|$), input-reflection ($|S_{dd11}|$), and common-mode suppression ($|S_{cc21}|$) responses of the proposed balanced wideband BPF with Z_m = 116.2 Ω, Z_{m1} = 33.3 Ω, and Z_{s1} = Z_{s2} = 55.112 Ω when N_m = N_s =1.

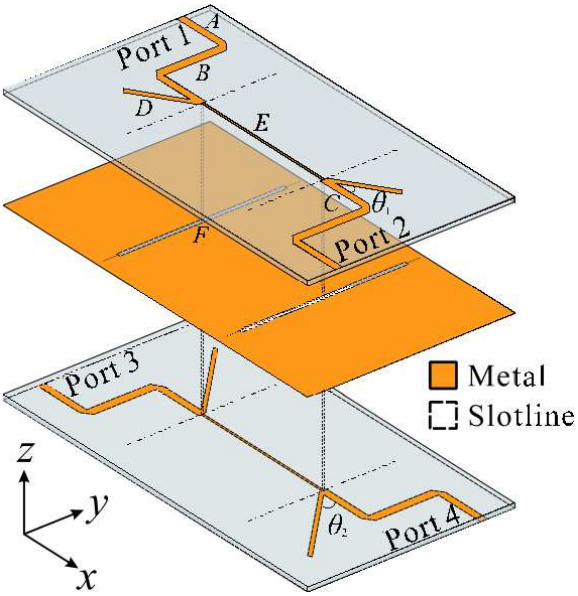

Fig. 3 Layout of the designed balanced wideband high-selectivity BPF prototype in a two-layered substrate [dimensions: L_A = 17.18, L_B = 30, L_C = 17, L_D = 21.8, L_E = 46.86, L_F = 74.59, W_A = W_B = W_C = 1.82, W_D = 1.6, W_E = 0.22, W_F = 0.38, (unit: mm), and θ_1 = θ_2 = 45°].

53.2796 Ω, and Z'_{s1} = Z'_{s2} = 90.205 Ω to make the EM-simulated response to closely match the theoretical one. Based on these two sets of impedance values, N_m = 0.975 and N_s = 0.782 are extracted. Moreover, due to the mutual-coupling effect existing between the feeding lines and the shunt open-circuit-ended stubs, the value of Z_{m1} was finely tuned to compensate it. Fig. 4 depicts the simulated and measured responses, as well as the photograph of the assembled prototype. A fairly-close agreement between the simulated and measured results is obtained. The measured metrics of the differential response are as follows: center frequency of 4.015 GHz, 3-dB fractional bandwidth of 38.06%, in-band minimum power insertion loss of 0.947 dB, and stopband-power-attenuation levels above 20 dB from 1.19 to 6.95 GHz. The common-mode suppression levels are above 20 dB from 2.075 to 5.588 GHz.

IV. Conclusion

A two-layered balanced wideband BPF with high filtering selectivity has been presented and its operational principle has been discussed. Based on the engineered differential-mode circuit, a fifth-order wideband BPF with sharp roll-off response is achieved. Furthermore, common-mode suppression levels higher than 20 dB for the entire frequency range of the differential-mode passband are obtained. Finally, a balanced wideband BPF prototype has been manufactured in microstrip technology and tested to verify the suggested design concept.

Acknowledgment

This work has been supported in part by the GOT ENERGY TALENT (GET) fellowship programme cofunded by the EU as part of the H2020-MSCA-COFUND programme under Grant Agreement number 754382 and in part by the Spanish Ministry of Economy, Industry, and Competitiveness (State Research Agency) under Project PID2020-116983RB-I00.

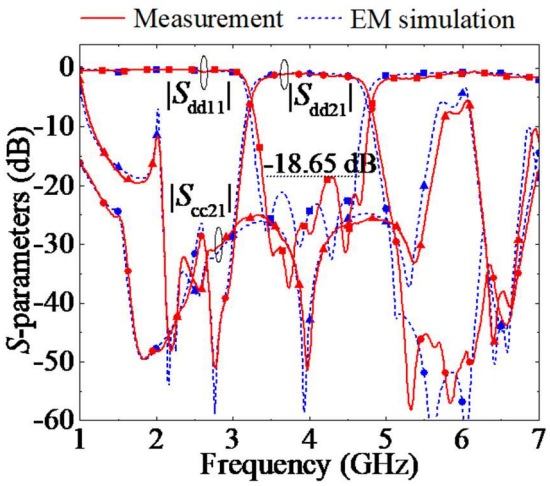

(a)

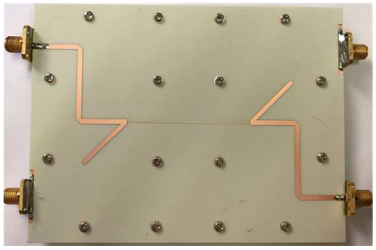

(b)

Fig. 4 Frequency responses of the fabricated two-layered balanced wideband high-selectivity BPF prototype in Fig. 3. (a) Simulated and measured differential-mode power transmission ($|S_{dd21}|$), input-reflection ($|S_{dd11}|$), and common-mode suppression ($|S_{cc21}|$) responses. (b) Photograph (top/bottom view) of the assembled BPF prototype.

References

[1] F. Martin, L. Zhu, J.-S. Hong, and F. Medina, *Balanced Microwave Filters*, 1st ed. New York, NY, USA: Wiley, 2018.

[2] T. B. Lim and L. Zhu, "Highly selective differential-mode wideband bandpass filter for UWB application," *IEEE Microw. Wireless Compon. Lett.*, vol. 21, no. 3, pp. 133–135, Mar. 2011.

[3] X.-H. Wu, Q.-X. Chu, and L.-L. Qiu, "Differential wideband bandpass filter with high-selectivity and common-mode suppression," *IEEE Microw. Wireless Compon. Lett.*, vol. 23, no. 12, pp. 644–646, Dec. 2013.

[4] X.-H. Wang, Q. Xue, and W.-W. Choi, "A novel ultra-wideband differential filter based on double-sided parallel-strip line," *IEEE Microw. Wireless Compon. Lett.*, vol. 20, no. 8, pp. 471–473, Aug. 2010.

[5] W. J. Feng and W. Q. Che, "Novel wideband differential bandpass filters based on T-shaped structure," *IEEE Trans. Microw. Theory Tech.*, vol. 60, no. 6, pp. 1560–1568, Jun. 2012.

[6] J. J. Sánchez-Martínez and E. Márquez-Segura, "Analytical design of wire-bonded multiconductor transmission-line-based ultra-wideband differential bandpass filters," *IEEE Trans. Microw. Theory Techn.*, vol. 62, no. 10, pp. 2308–2315, Oct. 2014.

[7] X. Guo, L. Zhu, K.-W. Tam, and W. Wen, "Wideband differential bandpass filters on multimode slotline resonator with intrinsic common mode rejection," *IEEE Trans. Microw. Theory Techn.*, vol. 63, no. 5, pp. 1587–1594, May 2015.

[8] L. Yang, L. Zhu, W.-W. Choi, K.-W. Tam, and R. Zhang, "Compact wideband microstrip-to-microstrip vertical transition with extended upper stopband," *Int. J. RF Microwave CAE*, vol. 28, no. 4, e21228, Dec. 2017.

[9] L. Yang et al., "Novel multilayered ultra-broadband bandpass filters on high-impedance slotline resonators," *IEEE Trans. Microw. Theory Techn.*, vol. 67, no. 1, pp. 129–139, Jan. 2019.